CONF-8809202--2

EXPERIMENTAL STUDIES OF U-Pu-Zr FAST REACTOR FUEL PINS IN EBR-II

R. G. Pahl, D. L. Porter, C. E. Lahm and G. L. Hofman‡

CONF-8809202--2

DE89 003628

Argonne National Laboratory

Experimental Breeder Reactor-II Division

P.O. Box 2528

Idaho Falls, ID 83403

and

‡Argonne National Laboratory

9700 S. Cass Avenue

Argonne, IL 60439

Submitted for publication in the proceedings of the Fall 1988 AIME Meeting, "Symposium on Irradiation-Enhanced Materials Science", Chicago, IL

EXPERIMENTAL STUDIES OF U-Pu-Zr FAST REACTOR FUEL PINS IN EBR-II*

I. INTRODUCTION

The Integral Fast Reactor (IFR) is a generic reactor concept under development by Argonne National Laboratory. Much of the technology for the IFR is being demonstrated at the Experimental Breeder Reactor II (EBR-II) on the Department of Energy site near Idaho Falls, Idaho. The IFR concept relies on four technical features to achieve breakthroughs in nuclear power economics and safety: (1) a pool-type reactor configuration, (2) liquid sodium cooling, (3) metallic fuel, and (4) an integral fuel cycle with on-site reprocessing.[1] The purpose of this paper will be to summarize our latest results of irradiation testing uranium-plutonium-zirconium (U-Pu-Zr) fuel in the EBR-II.

II. BACKGROUND

In order to better appreciate the materials aspects of our fuel tests, a brief description of the key design features will be given. The ultimate criteria for fuel pin design is the overall integrity up to the planned lifetime or target burnup of irradiation. Here burnup refers to the fraction

*Work supported by the U.S. Department of Energy, Civilian Reactor Development, under Contract W-31-109-Eng-38.

of total heavy metal constituents (U+Pu) which have undergone fission and hence transferred thermal power to the sodium reactor coolant medium flowing around the pins. Achievement of burnups near 15 at.% are desirable for large-scale commercialization of liquid-metal reactors (LMR). Figure 1 illustrates the key design features of a generic metallic fuel pin along with some typical specifications for actual IFR test pins irradiated in this study. The fuel itself is a solid cylinder which has been injection-cast into quartz molds and loaded into the cladding jacket with no thermo-mechanical pretreatment required. The as-cast density of these alloys is ~15.8 g/cm^3. Sodium fills the annulus around the slug and provides a high conductivity heat path to the cladding prior to fuel slug swelling. The plenum space (initially filled with inert gas) above the fuel slug is provided to contain the large volume of stable fission gas (Xe/Kr) which is produced in these fuel slugs at the rate of ~16 cm^3 (STP) per % burnup. The ends of the jacket are hermetically sealed with an automated tungsten inert gas welder and a helical wire is welded in place to maintain pin spacing and mix coolant flow upward through the close-packed hexagonal pin bundle (so-called subassembly) during irradiation.

The key phenomena which are significant in controlling fuel pin behavior and reliability are summarized in Table I. Each of these effects will be described in more detail in the Results sections which follows.

Most of the irradiation tests performed to date have been of a "proof test" nature to demonstrate the high burnup potential of the reference metallic fuel system, with a few follow-on experiments designed to understand specific performance issues on a somewhat more basic level. A family of

uranium-base alloys has been chosen as the reference design fuel for the IFR concept. The base alloy, U-10Zr, (unless otherwise stated all compositions are in weight percent) is the likely start-up fuel of choice. Subsequent reprocessing cycles utilizing the plutonium bred from U^{238} in blanket subassemblies will eventually lead to a maximum equilibrium content on the order of 20-25% plutonium. Thus, the IFR concept is a closed cycle, with no subsequent off-site supply of fissionable material necessary. The reprocessing cycle uses electro-refining methods recently developed[2] with liquid cadmium anodes and fused chloride salts to extract the pure uranium and plutonium from the spent fuel. Remote manufacture in shielded hot-cell facilities of fresh fuel pins completes the cycle.

Testing of fuel alloys with starting composition given by U-xPu-10Zr (X=0,3,8,19,22, and 26%) thus provides a broad basis for demonstrating and understanding fuel behavior at all stages in the reactor cycle. The zirconium content (10 wt % ~22.5 at.%) was chosen to assure adequate chemical compatibility at the fuel/clad surface and an improved solidus temperature which is especially important for the high plutonium alloys. This increase in solidus temperature amounts to ~13°C for each percent of zirconium present for a 20% plutonium alloy.

Cladding alloy development programs both here and abroad have led to a progression of cladding alloys for liquid metal reactor applications. Early on, the cladding materials of choice were rather low-alloy austenitic stainless steels. A progression from 304 (18 Cr-8 Ni) to 316 (18 Cr-12 Ni-2.5 Mo)

TABLE I - KEY PEHNOMENA THAT CONTROL FUEL PERFORMANCE

PHENOMENA	EXPERIMENTAL OBSERVATIONS	CONSEQUENCES
Fuel Swelling	Irradiation Growth and Grain-Boundary Tearing; Xe/Kr Bubble Growth; Solid Fission Product Accumulation; Alloy and Burnup Rate Effects	Reactivity Loss; Rate of Gas Release; Fuel/Clad Interaction Stresses; Thermal Conductivity Loss
Fuel Constituent Migration	U/Zr Interdiffusion; Critical Pu Threshold	Lowered Solidus; Complexities of Properties Modeling
Fuel/Cladding Chemical Interaction	Penetration into Cladding by U, Pu, and Lanthanide Series Fission Products; Diffusion of Cladding Constituents into Fuel; Extensive Nickel Loss in Austenitics	Cladding Wall Thinning; Ductility Degradation of Interaction Layer in Cladding; Eutectic Composition Approached in Fuel
Cladding Deformation	Irradiation/Thermal Creep by Fission Gas Pressure Loading; Some Fuel Contact Pressure Loading; Void Swelling in Austenitics	Stress-Rupture Lifetime Determines Ultimate Burnup Achieved; High Cladding Strains can Lead to Element/Bundle Interaction Stresses

to D9 (14 Cr-15 Ni-1.5 Mo-.2 Ti) was implemented over the past 20 years in order to improve the void-swelling resistance of fuel cladding. Cold-working was also adopted for similar reasons. However, as longer-lived reactor cores were designed, and intercomponent clearances remained fixed, irradiation-induced swelling limited the use of 300 series steels. At very high neutron fluences, even the most resistant alloys eventually showed unacceptable dimensional instabilities associated with void selling. All of these austenitic steels eventually swell (by volume) at the rate of ~1%/dpa or ~5%/10^{22} neutrons/cm^2 (E > .1 Mev) once an incubation period (dependent on the alloy) is exceeded.

To mitigate this problem, a third class of alloys based on the ferritic/martensitic structure has been developed. The leading candidate of this type today is HT-9, an Fe-12 Cr-1 Mo alloy used in the tempered condition. With essentially zero swelling up to ~100 dpa (~20x10^{22} neutrons/cm^2) the use of this class of materials has become widespread. EBR-II irradiation of IFR test fuel pins has employed three types of cladding: austenitic (20% CW 316), modified austenitic (20% CW D9) and tempered martensitic alloys (HT-9) to provide reactor core designers with a broad data base with which to work.

The neutronic environment of EBR-II and typical operating conditions for the IFR fuel tests are given in Table II. Reactor operation consists of round-the-clock cycles of ~50-100 days followed by shutdown periods for maintenance and refueling which lasts ~5-10 days. The post-irradiation examinations (PIE) of the fuel are carried out some 30-60 days after removal from EBR-II, to allow the high fission product gamma heat to decay to levels

TABLE II

TYPICAL PEAK OPERATING CONDITIONS OF THE IFR FUEL TESTS

Fuel Centerline Temperature, °C	670, 805*
Cladding Inside Wall Temperature, °C	595
Subassembly Inlet Sodium Temperature, °C	370
Subassembly Outlet Sodium Temperature, °C	500
Fuel Pin Power, W/cm	480
Total Neutron Flux, 10^{15} n/cm^2-s	2.5
Fast Neutron Flux (E>.1 Mev), 10^{15} n/cm^2-s	2.2
U^{235} Fission Rate, 10^{12} fissions/g-s	9.0
Pu^{239} Fission Rate, 10^{12} fissions/g-s	10.4
Burnup Rate, 10^{-7}%/s	2.3

* Calculated for U-19Pu-10Zr fuel at ~2% burnup[3], all other data for fresh fuel.

amenable for subassembly transfer. All PIE is performed in shielded facilities at the Idaho site adjacent to the reactor or at the hot-cell facilities at Argonne's site in Illinois.

III. RESULTS

A. Fuel Swelling

Because our irradiation tests were designed to demonstrate metallic fuel burnup capability and not fundamental research on irradiation damage, a precise description of swelling mechanisms in our fuel samples has not yet been attempted. Moreover, no attempts have been made to control swelling by alloying or heat treatment because, as we can now demonstrate, high burnup reliability in our fuel system is readily achievable.

Four major mechanisms for macroscopic fuel swelling can be identified:

1) Irradiation growth
2) Grain boundary mechanical cavitation
3) Fission gas bubble growth
4) Solid fission product accumulation

The anisotropic irradiation growth (i.e., shape change) of single crystals of orthorhombic alpha uranium has been recognized and fairly well understood since the 1960's. Shape changes involving [010] elongation and [100] shrinkage has been satisfactorily explained by the anisotropic condensation of interstitial and vacancy loops in the lattice. In a random polycrystal mismatched growth stresses develop at grain boundaries which

caused plastic flow or cavitation depending on the grain size and temperature. Fission gas diffusion to these cavities may assist the process but the driving force is mainly the anisotropic growth of individual grains. Complicating this process would be the presence of a preferred grain orientation or texture, induced by stress or temperature gradients during manufacture or in-reactor operation.

Fission gas bubble growth can also be a major contributor to swelling, particularly at high temperatures where their coarsening and coalescence is favored. Because the fission yield of noble gases is high (25 % for Xe + Kr), supersaturation is quickly reached at low burnup and the gas precipitates as nominally spherical bubbles. Their internal pressure is equilibrated with the surface energy and external pressure by ingestion of vacancies which are mobile and readily available as irradiation defects.

Solid fission products (mainly Mo, Ru, Zr, Pd and the lathanide series) accumulate inexorably with burnup as substitutional atoms or precipitates and account for atomic volume increases of ~2% per % burnup.

Grain boundary cavitation occurs in fuel slugs near the outer surface where the temperature favors alpha uranium formation (400° to 650°C). Though uncertainties in the ternary phase diagram for U-Pu-Zr exist, the zirconium probably exists in the hexagonal delta phase (UZr_2) or the tetragonal zeta phase depending on Pu concentration and temperature. Some of the zirconium is also tied up in Zr-rich globular precipitates stabilized by O,C, and N. We believe the "marble-cake" structure in Fig. 2 has been caused by the

cavitational mechanism. The fuel shown is U-8Pu-10Zr irradiated to 10% burnup. Closer inspection of these types of voids show many of them to be partially filled with precipitates. Electron microprobe analysis of sibling fuel has shown this material to be lanthanide- rich (La, Ce, Pr and Nd) fission product precipitates which have begun to accumulate in quantities easily observable by optical techniques.

Fission gas bubbles have also been observed in our fuel tests, particularly at slug centerline where the operating temperatures insure single-phase gamma (B.C.C.) formation. A good example of single and coalesced fission gas bubbles in U-19Pu-10Zr fuel at 2% burnup is shown in Fig. 3. The smooth isotropic shape of the bubbles suggests they are true fission gas bubbles, possessing none of the fracture-surface like morphology of the grain boundary cavities discussed above.

In addition to the microscopic examples of fuel swelling presented in the photomicrographs, we have also used neutron radiography and immersion density to measure the macroscopic swelling levels in our fuel. Figure 4 shows the axial growth behavior of U-10Zr fuel as a function of burnup for comparable operating conditions out to 14% burnup. The shape of the swelling curve shown is typical for all of our irradation tests, with a summary of our general observations given below:

1. Rapid "breakaway" swelling in all alloys tested occurs at low burnup and continues (15 to 25% $\Delta V/V_o$/% burnup) until cladding restraint occurs at ~2% burnup.

2. In all alloys tested (U-xPu-10Zr x=0,3,8,19,22,26) the average radial swelling strains ($\Delta d/d_o$) exceed the axial strain ($\Delta l/l_o$) by factors of 2-3. We are currently investigating the possibilities of texture in our as-cast fuel by neutron diffraction. Experimental evidence[4] has shown that a positive growth texture [010] is produced perpendicular to the temperature gradient in uranium Jominy tests. Because directional solidification in our injection casting furnace proceeds axially from top-to-bottom, a radial growth texture which exists during irradiation in the alpha phase region cannot be discounted.

3. Increasing the plutonium content causes the ultimate swelling level at high burnup to decrease as shown in Fig. 5.

4. The plateau in axial growth of U-19Pu-10Zr fuel (but not U-10Zr or U-8Pu-10Zr) was apparently dependent on fission rate. Slow burnup rate fuel experienced approximately twice the axial growth of the fast burnup rate fuel (4.5×10^{13} U^{235} fissions/cm^3-s vs 8.8×10^{13} U^{235} fissions/cm^3-s). Concomitant chemical restructuring (Zr migration) in the high fission rate fuel only, (prior to cladding contact), and the associated presence of transverse and pie-shaped radial cracks, severely complicates our understanding of this data set. It may be that the growth stresses between individual grains which rise more rapidly in the high-fission-rate fuel are relieved by the cracking. Thus a creep ductility dependence on strain (i.e., swelling) rate, may be implied.

B. Fission Gas Retention and Release

Since cladding creep responds principally to the pin's internal gas pressure, fission gas release behavior is an important parameter in controlling the probability of pin breach during steady state and transient reactor operation.

Numerous computer codes have been written to mechanistically model this complex behavior in fast and thermal reactor fuel. Treatment of gas behavior in oxide fuel [5] as well as metallic fuel[6] can be found in the literature. The latter works includes the effects of single gas atom diffusion and trapping, bubble nucleation and resolution and can account for the variation of the effective diffusion coefficient with burnup.

Several general conclusions regarding fission gas retention/release has come out of their modeling efforts[7]:

1. The quantity of gas which percolates into the pin plenum (and hence plenum pressure) shows a nearly linear dependence on burnup once the initial incubation transient (~0.5% burnup) has passed.

2. Fractional gas release (i.e., the fraction of the theoretical gas production which is released to the plenum) increases rapidly with burnup and eventually asymptotically approaches 100%.

3. Within a typical fuel slug, the axial variation of retained fission gas along the fuel column is small, suggesting mild dependence on local fuel temperature and diffusion distance from the plenum.

Figure 6 shows the gas release data as a function of burnup from four experimental subassemblies which had similar operating histories. The test contained fuel alloys of U-10Zr, U-8Pu-10Zr and U-19Pu-10Zr. The data was obtained by puncturing the plenum with a laser, measuring the pressures and back-fill volumes and assuming ideal gas behavior.

The predicted incubation period and linear release rate with burnup has been experimentally verified. It is clear that while the details of swelling and microstructure varies greatly with alloy composition, the gas release behavior may be a general function of operating conditions only (i.e., pin power, plenum volume, etc.). A least squares fit to all of the data yielded a fractional release correlation plotted with the raw data in Fig. 7. The functional form is as expected by theory with approximately 80% gas release for typical goal burnups of -15%.

Retained fission gas was also measured on sibling pins at various elevations along the fuel column. Figure 8 shows the data from a U-19Pu-10Zr fuel slug which had been irradiated to 11.9% peak burnup. The slug was sectioned and declad in 6.3 cm samples and dissolved in an HCl, HNO_3 and HF acid bath. The released gas was collected in a charcoal trap and concentrated by cryo-pumping into a sample chamber for analysis by isotopic dilution mass-

spectrometry. A relatively flat profile for both xenon and krypton resulted, suggesting similar percolation rates with a mild temperature dependence.

C. Fuel/Cladding Chemical Interaction (FCCI)

Fuel/cladding chemical interaction (FCCI) involves the interdiffusion of fuel and cladding constituents at operating temperatures. Specifically, the interdiffusion has been characterized by diffusion of Fe and Ni, when available as a cladding constituent, into the fuel with corresponding diffusion of lanthanide fission products (La, Ce, Nd, Sm, Pr) into the cladding. Figure 9 shows typical metallography of the fuel/cladding interface region where the interaction has occurred.

The interdiffusion is also characterized by diffusion of cladding alloying pins into the body of the fuel. At minor degrees of interaction, metallography does not often show the area of interaction in the fuel. The interaction in the cladding, however, follows a very defined interaction front, leaving a layer of cladding which contains nearly 20 wt % of the lanthanides. This layer is clearly shown in Fig. 9 for U-19Pu-10Zr clad in D9 stainless steel at 11.9% peak burnup.

Consequences of FCCI involve modification of the mechanical properties of the cladding by lanthanide intrusion, and lowering of the fuel melting point as it is alloyed with Fe and Ni (Cr does not appear to diffuse into the fuel to any significant extent). The lowering of the fuel melting point does not

significantly alter steady-state fuel operation as the U-Fe eutectic is 715°C which is well above normal fuel temperatures near the cladding surface, the only location where large concentrations of cladding constituents approaching the UFe_2/U_6Fe eutectic may be present. The effect does limit the off-normal capabilities of the fuel pin, in that the cladding can be penetrated rapidly if temperatures are elevated to the point where molten phase occurs. Reactor designs are therefore limited to ensure that such cladding penetration is not likely to occur.

The incorporation of lanthanide fission products in a cladding layer is of more importance to steady-state fuel performance. The interaction layer has been found to extend to ~0.1 mm at 10 at.% burnup. The lanthanides harden and embrittle the cladding as indicated by the hardness indent sizes in Fig. 9. Hardness values in the reacted layer have been measured as high as ~1100 DPH vs. ~325 DPH in the unreacted D9 cladding bulk. To date, fuel performance modeling has been forced to assume that mechanical integrity of the FCCI layer has been lost entirely. There is some evidence that this is a very conservative assumption and tests are underway to measure the properties of this layer, by creating them in the laboratory, so as to strengthen the accuracy of fuel performance codes.

D. Fuel Restructuring

Figure 10 shows a cross section of an irradiated U-19Pu-10Zr pin at ~3 at.% burnup. The obvious radial zones in the fuel have been created by fuel restructuring, combining radially-dependent fuel swelling behavior and

fuel constituent segregation. The light-colored ring of fuel has only 2 wt % of Zr and is enriched in U, resulting in an overall composition of U-19Pu-2Zr. The other zones are enriched in Zr at the expense of U. Fuel restructuring has been observed as mid-radius Zr-depleted zone, or a two-zone structure where the depleted region occurs at the center of the fuel, Fig. 11. These types of restructuring are, however, limited to fuel compositions containing 15 wt % Pu or greater; fuel containing 8 wt % Pu or less does not show significant restructuring except for a rather homogeneous development of fission gas bubbles and grain boundary cavities.

The fuel performance consequences of restructuring are primarily concerned with the lowering of fuel solidus temperatures in Zr-depleted areas. The solidus of the U-19Pu-2Zr zone shows in Fig. 10 is 1032°C, while the solidus temperature of the nominal U-19Pu-10Zr fuel is 1126°C. These changes are not significant to steady-state fuel performance, and off-normal performance is limited more by FCCI effects and cladding mechanical properties rather than solidus changes.

The reasons for fuel restructuring in the form of constituent migration are not yet well known. However, models based upon segregation driven by chemical activity gradients in the fuel are most widely accepted. The theories are based on the fact that radial temperature gradients create radial zones which represent ternary phase fields. The particular phase fields created incorporate phases with varying Zr activities, and the variations drive diffusion. Recent evidence has indicated that the radially-dependent fuel swelling behavior precedes the constituent migration, and therefore the

swelling process itself may contribute to the segregation phenomenon. More work is needed to produce a clear explanation for the behavior as it is now clear that thermodynamic and diffusion properties of the U-Pu-Zr system are needed as well as a more precise description of the U-Pu-Zr ternary phase equilibria than now exists[8].

E. Cladding Deformation

Cladding deformation is the result of irradiation-induced void swelling and creep, and thermal creep. The creep is driven by the stresses imposed by released fission gas and fuel/cladding mechanical interaction (FCMI) phenomena. The former can be reduced by providing a larger plenum and lowered cladding temperature but compact core lengths and high coolant outlet temperature are economically favorable. Fuel cladding contact stresses can be minimized by maintaining a low (<75%) smear density (defined by the cross-sectional area of the fuel slug/the internal cladding cross-section) which guarantees a spongy fuel microstructure with open porosity. Previous studies[9] of metallic fuel behavior showed that FCMI was below detectable levels (to 8% burnup) in previous metal fuel designs using solution-annealed 316 SS. To date, the tests of IFR fuel clad in advanced alloys have shown no definitive evidence for FCMI, due to the low levels of total strain measured. The important point is that no unexpected large cladding strain which would affect pin reliability have been observed in D9 clad pins at ~15% burnup or HT-9 clad pins at 11% burnup. At higher fuel burnup (>20%),

however, the FCMI may become significant as solid fission products build-up, close off the interlinkage paths between pores and plenum, and effectively harden the fuel.

Figure 12 shows a comparison of cladding diameteral profiles between a D9 and an HT clad pin at similar exposures. It can be seen that while both profiles show low strains, the HT-9 performs in a superior manner in this regard. Within the uncertainties in property correlations and operating conditions, all of the strain can be accounted for by gas pressure loading and void swelling.

To illustrate the expected performance differences between austenitic, modified austenitics, and ferritic/martensitic steels, a set of calculations showed in Fig. 13 have been carried out. Three hypothetical pins were irradiated to 15% peak burnup with cladding alloys of 20% cold worked 316 SS, 20% cold-worked D9, and normalized- and tempered-HT-9, respectively. A constant peak cladding midwall temperature of 600°C and a linear hoop stress ramp rate of 8.9 MPa per % burnup were chosen. The peak fast fluence at core midplane was $\sim 14 \times 10^{22}$ n/cm^2 (70 dpa). The shape of the curves reflect the flux profile (chopped sine wave) and cladding temperature profile which increases almost linearly from left to right. The uppermost curve predicted for the 20% CW 316 pin would preclude its use to this burnup due to pin-pin or pin-subassembly interference. The middle curve shows the D9 pin at an acceptable level of strain but rapid swelling at increased exposure would be limiting. The lower curve for HT-9, which is essentially 100% cladding creep, illustrates why it is the alloy of choice for most long-life advanced reactor

designs. The limitation of HT-9 for cladding application is its high temperature strength. The onset of tertiary creep at ~650°C[10] and the rapid strain rates above 700°C require high temperature operation to be limited to short times.

IV. SUMMARY

Recent irradiation tests in EBR-II have provided experimental data on the performance characteristics of U-Pu-Zr, the reference Integral Fast Reactor (IFR) fuel type. While no serious barrier to high burnup performance has been observed in these demonstration tests, detailed mechanistic descriptions of the observed fuel swelling, gas release, fuel constituent redistribution, and fuel/clad chemical interaction are needed before steady-state and off-normal operation can be modeled completely. Future reactor and laboratory tests will be directed toward this effort.

ACKNOWLEDGEMENTS

This work has been sponsored by the U. S. Department of Energy, Civilian Reactor Development, under contract W-31-109-Eng-38.

REFERENCES

1. C. E. Till and Y. I. Chang: *Proceedings of the American Power Conference*, 1986, vol. 48, p. 688.

2. L. Burris, et al: *Transactions of the American Nuclear Society Annual Meeting*, 1988, vol. 56, p. 68.

3. M. C. Billone: Argonne National Laboratory, Argonne, IL, unpublished research, 1987.

4. K. R. Riggs and N. F. Neumann: MCW-1491, TID-4500, 40th Edition, Mallinckrodt Chemical Works, Weldon Spring, MO, April 1965.

5. M. H. Wood and J. R. Mathews: *J. Nuclear Materials*, 1980, vol. 91, p. 35.

6. M. C. Billone, et al: *Proceedings of the International Conference on Reliable Fuels for Liquid Metal Reactors*, Tucson, AZ, 1986.

7. E. E. Gruber and J. M. Kramer: Argonne National Laboratory, Argonne, IL, unpublished research, 1988.

8. D. R. O'Boyle and A. E. Dwight: *Proceedings of the 4th International Conference on Plutonium and Other Actinides*, Santa Fe, NM, 1970.

9. D. L. Porter, et al: *Proceedings of the International Conference on Reliable Fuels for Liquid Metal Reactors*, Tucson, AZ, 1986.

10. G. L. Fox: *Proceedings of the International Conference on Reliable Fuels for Liquid Metal Reactors*, Tucson, AZ, 1986.

FIGURE CAPTIONS

Figure 1 Key Design Features of a Typical Metallic Fuel Pin.

Figure 2 As-irradiated Microstructure of a U-8Pu-10Zr Fuel Slug Showing Cavitation in the Outer Region.

Figure 3 Typical Fission Gas Bubble Distribution in the High Temperature Gamma Phase Region.

Figure 4 Axial Fuel Slug Swelling Behavior of the U-10Zr Alloy.

Figure 5 The Effects of Plutonium Content on the High Burnup Levels of Axial Fuel Swelling.

Figure 6 Linear Fission Gas Release Behavior in Fuel Alloys of the Type U-xPu-10Zr, x=0,8,19.

Figure 7 Fractional Fission Gas Release Behavior in Fuel Alloys of the Type U-xPu-10Zr, x=0,8,19.

Figure 8 Fission Gas Retained in a U-19Pu-10Zr Fuel Slug Irradiated to ~12% Burnup.

Figure 9 Etched D9 Cladding Microstructure at ~12% Burnup Showing the Increased Hardness of the FCCI Layer.

Figure 10 As-polished Microstructure of a U-19Pu-10Zr Slug Irradiated to ~3% Burnup Showing the Zirconium Depleted Annulus at Mid-radius.

Figure 11 As-polished Microstructure of a U-19Pu-10Zr Slug Irradiated to 5.5% Burnup Showing the Zirconium Depleted Region at Fuel Centerline.

Figure 12 Comparison of D9 and HT9 Cladding Diametral Profiles After Burnups of 10-11% Burnup.

Figure 13 Calculations of Cladding Diametral Profiles of the 316 SS, D9, and HT9 Alloys After 15% Burnup.

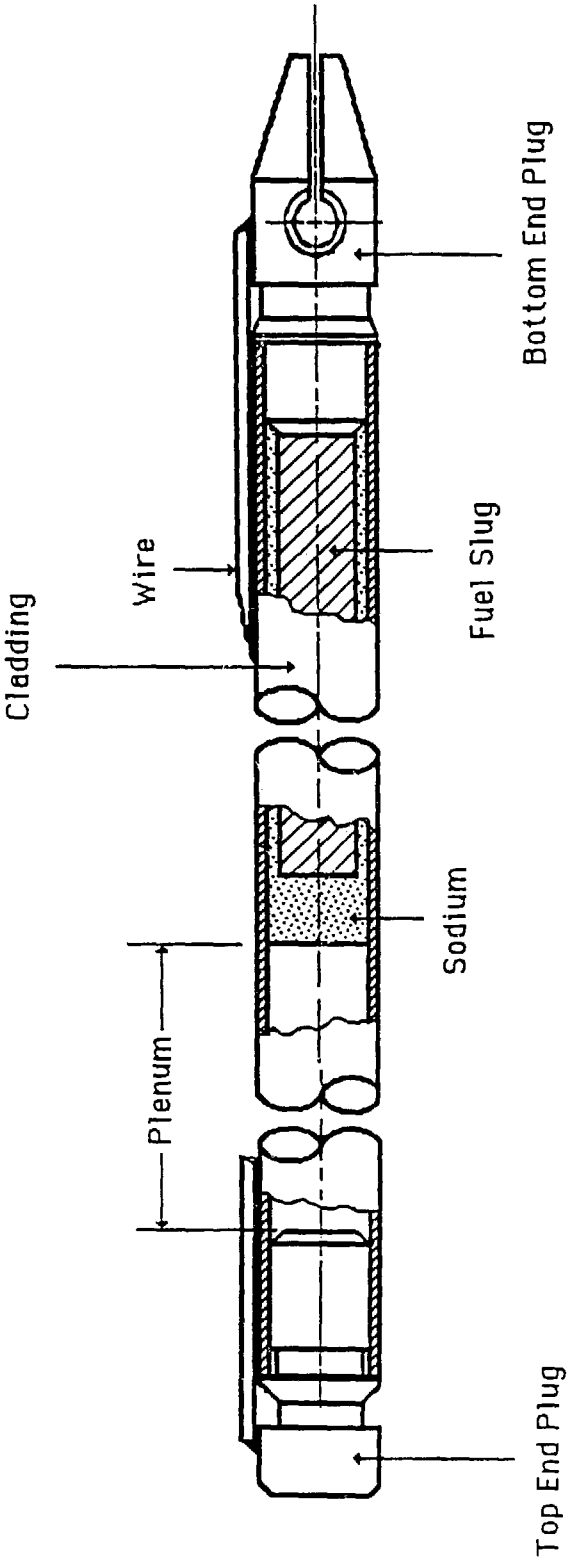

Figure 1 Key Design Features of a Typical Metallic Fuel Pin.

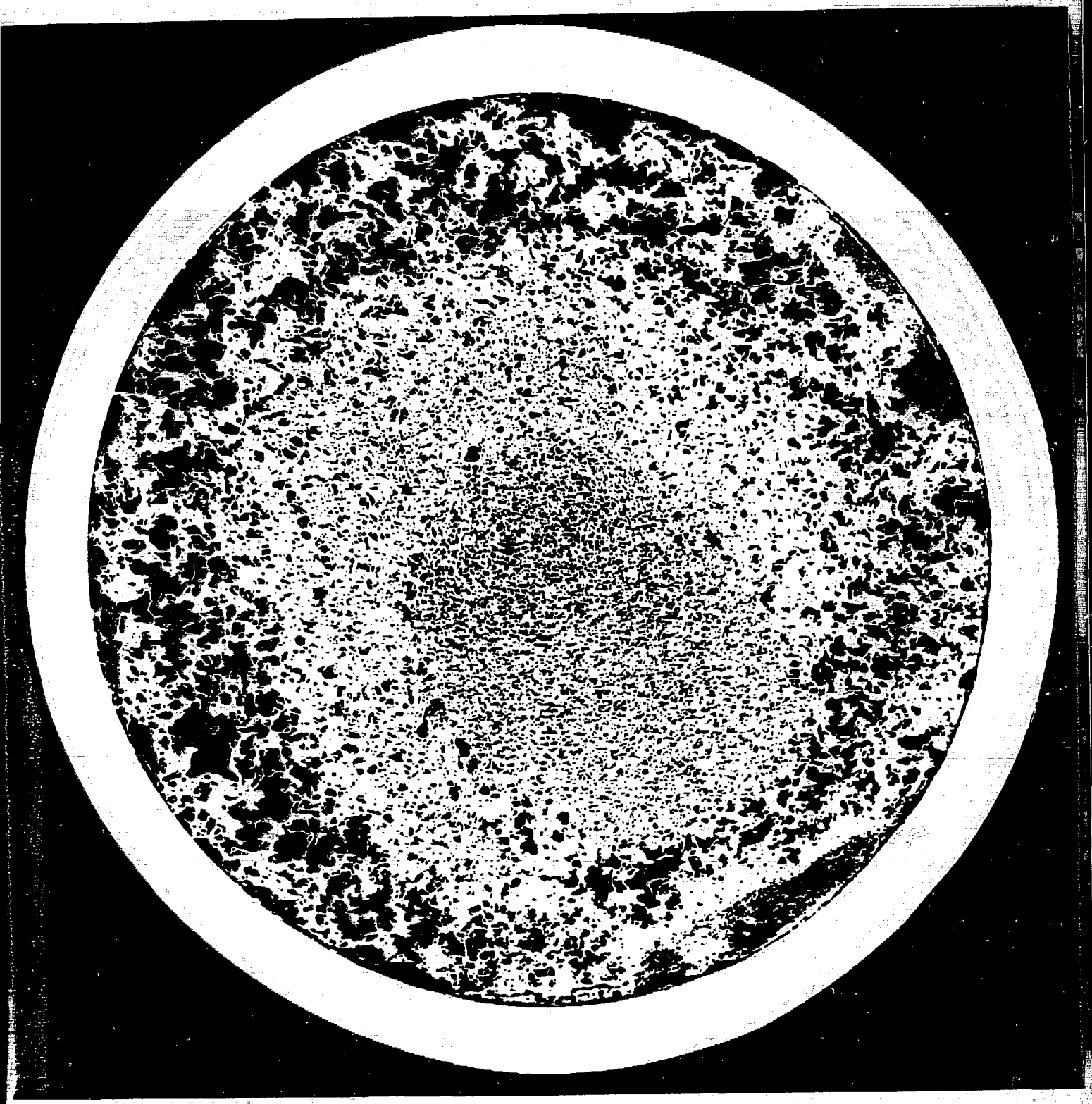

Figure 2 As-irradiated Microstructure of a U-8Pu-10Zr Fuel Slug Showing Cavitation in the Outer Region.

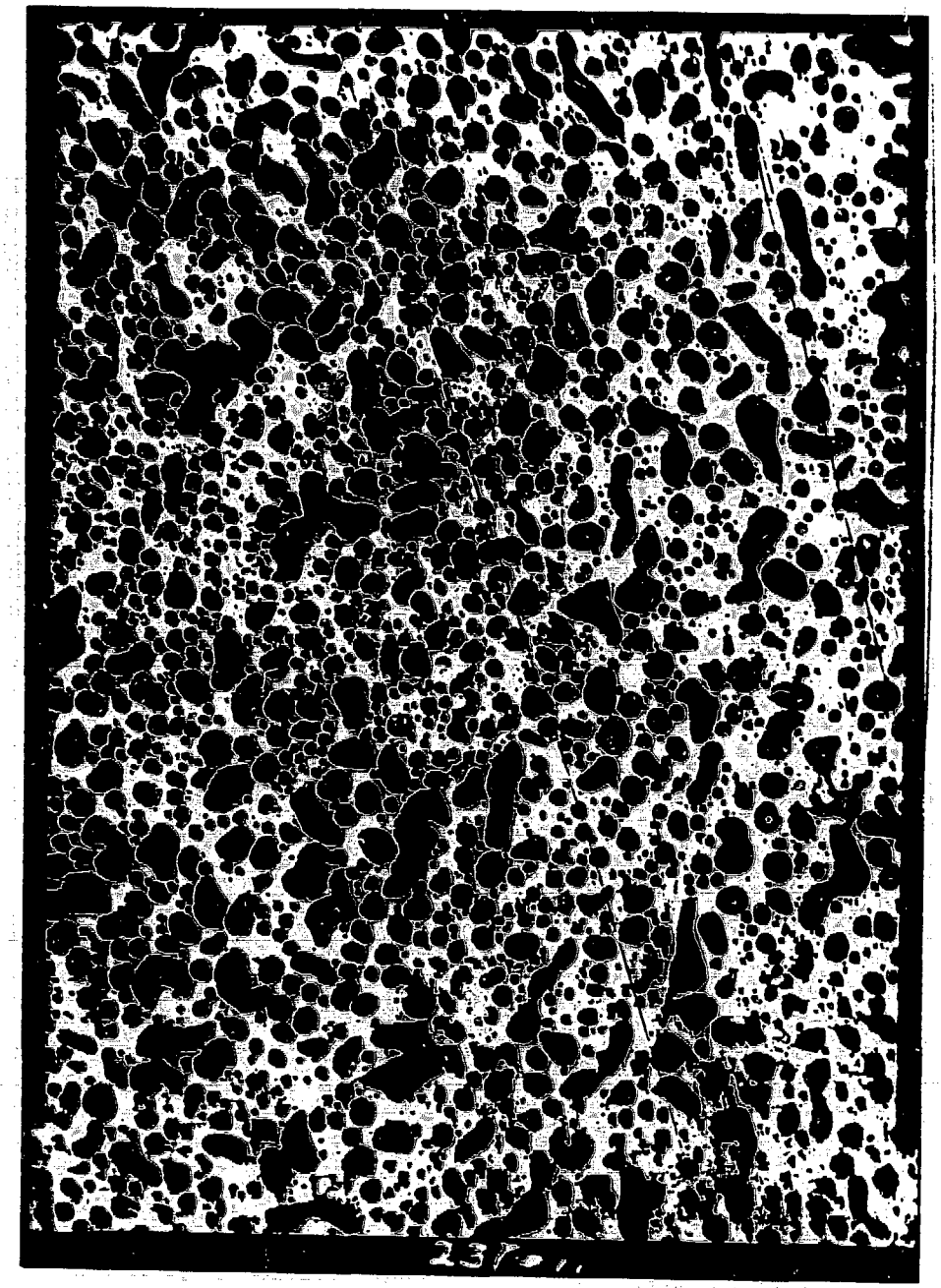

Figure 3 Typical Fission Gas Bubble Distribution in the High Temperature Gamma Phase Region.

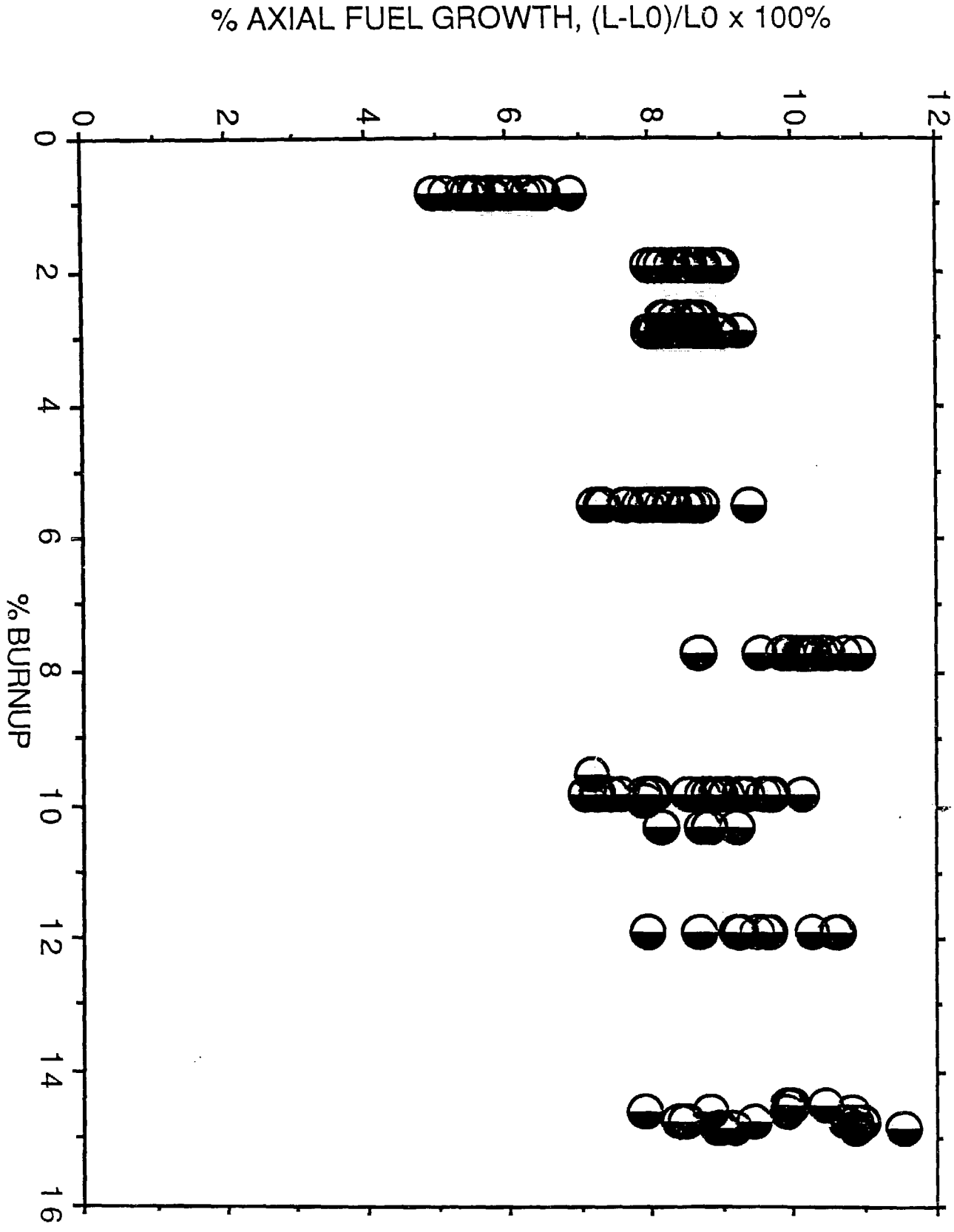

Figure 4 Axial Fuel Slug Swelling Behavior of the U-10Zr Alloy.

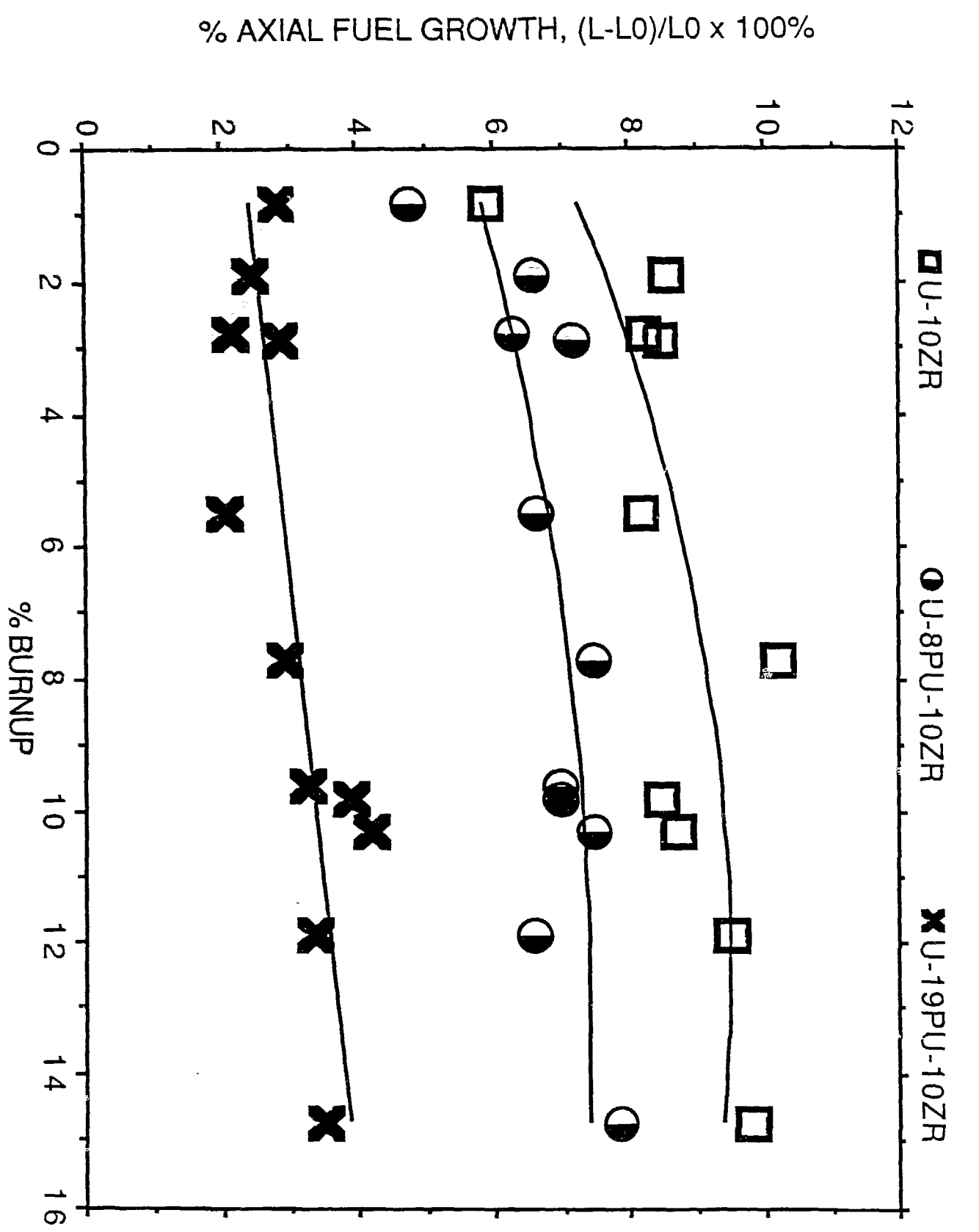

Figure 5 The Effects of Plutonium Content on the High Burnup Levels of Axial Fuel Swelling.

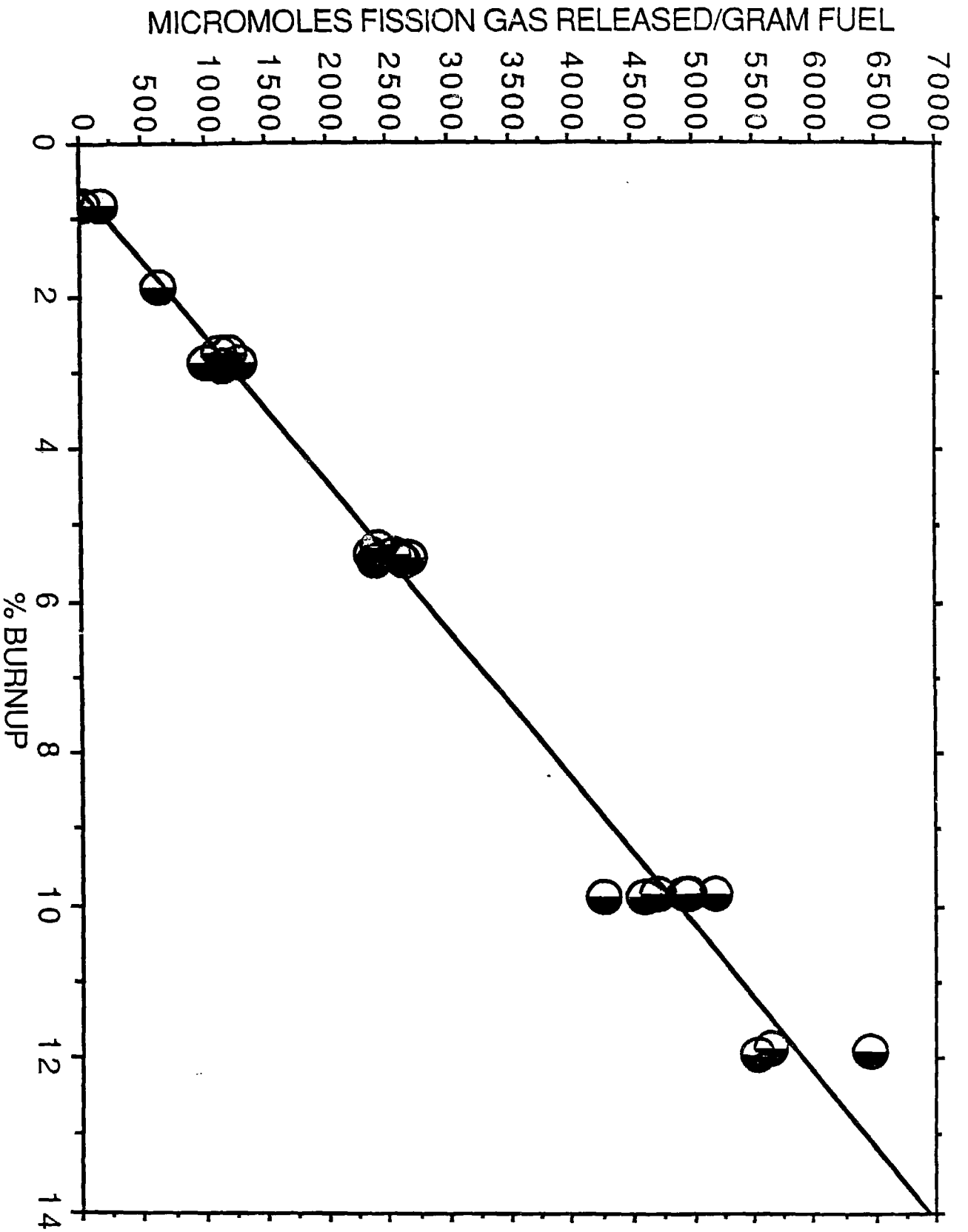

Figure 6 Linear Fission Gas Release Behavior in Fuel Alloys of the Type U-xPu-10Zr, x=0,8,19.

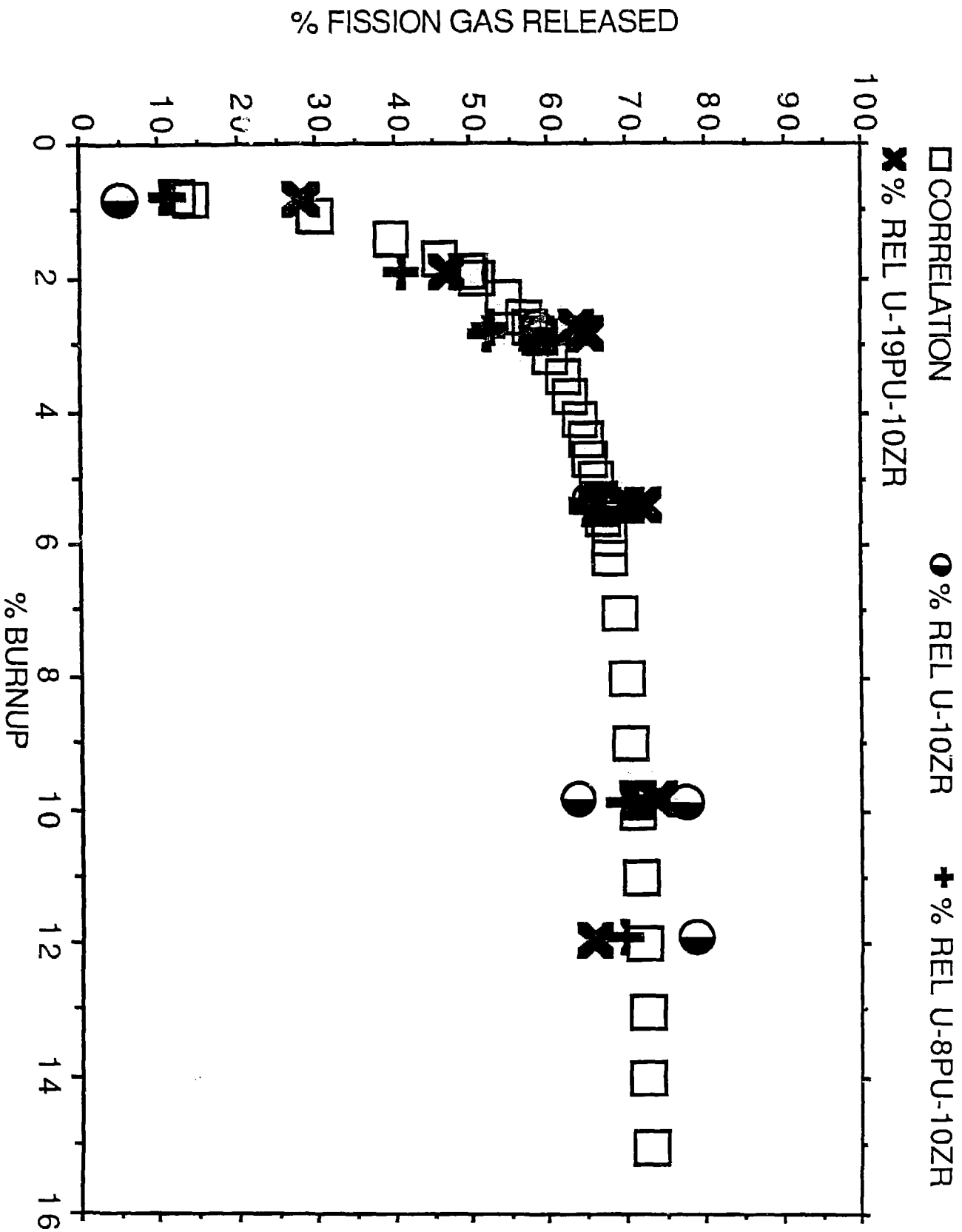

Figure 7 Fractional Fission Gas Release Behavior in Fuel Alloys of the Type U-xPu-10Zr, x=0,8,19.

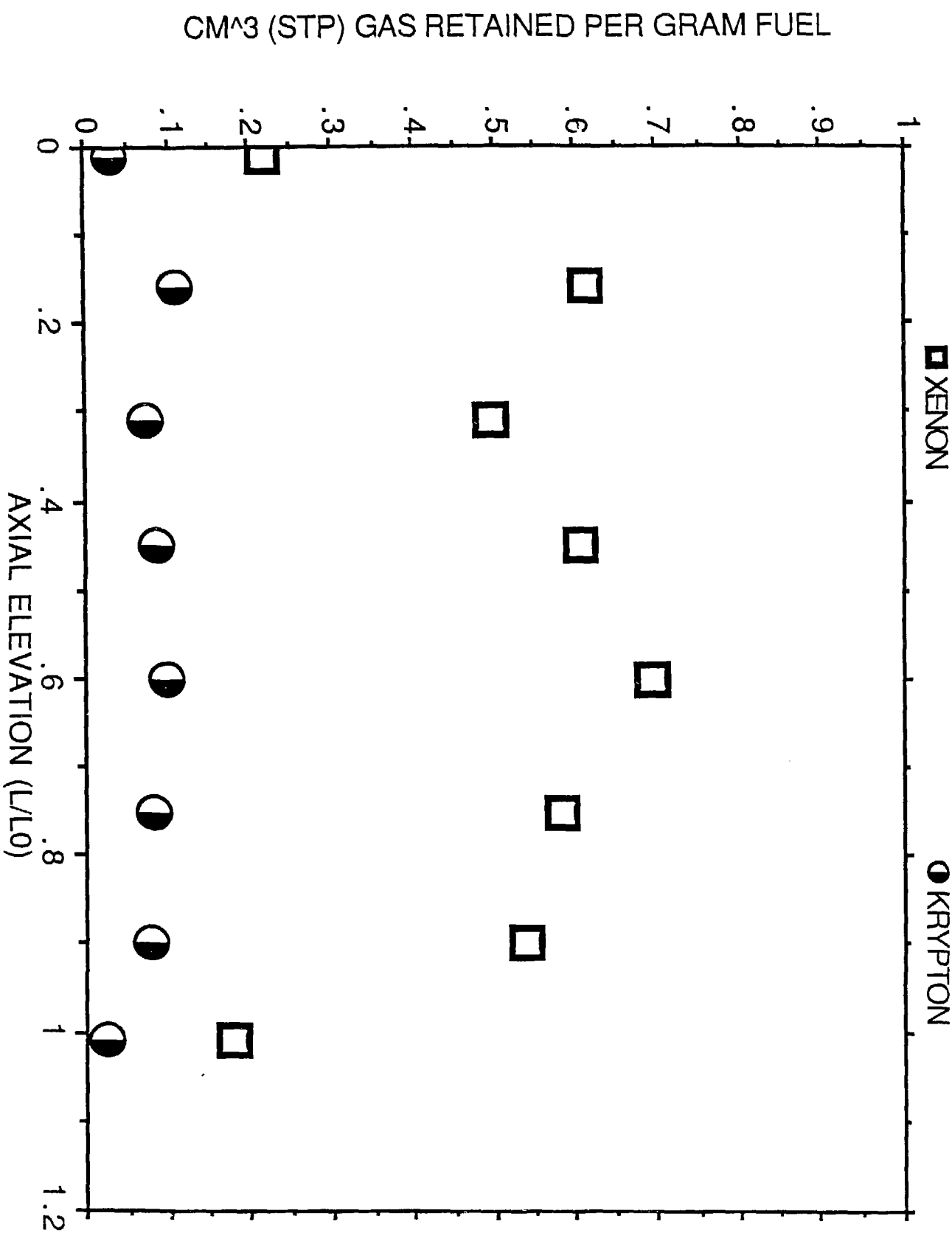

Figure 8 Fission Gas Retained in a U-19Pu-10Zr Fuel Slug Irradiated to ~12% Burnup.

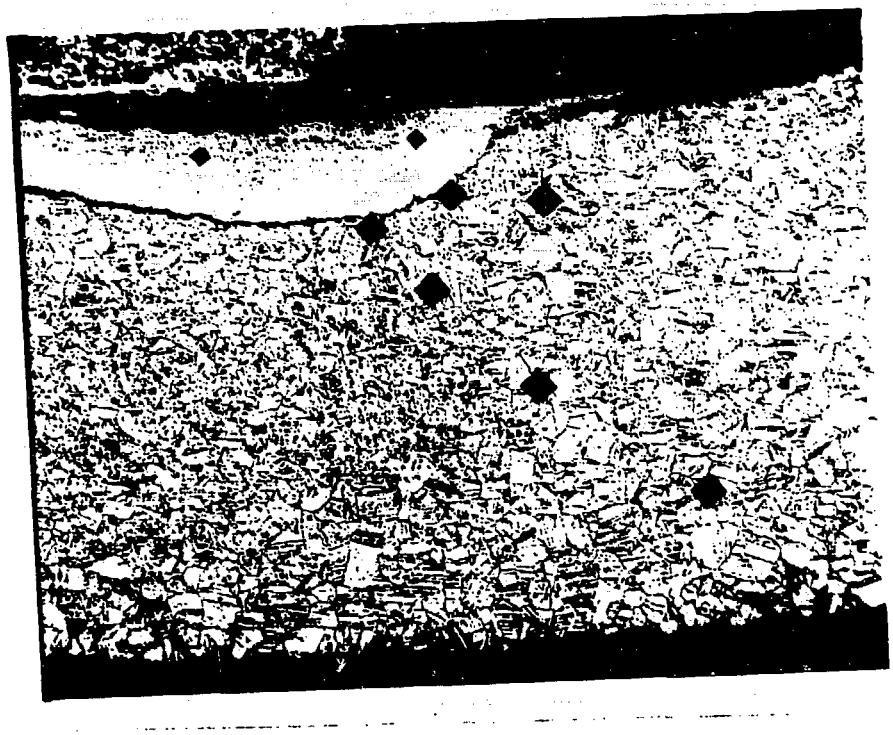

Figure 9 Etched D9 Cladding Microstructure at ~12% Burnup Showing the Increased Hardness of the FCCI Layer.

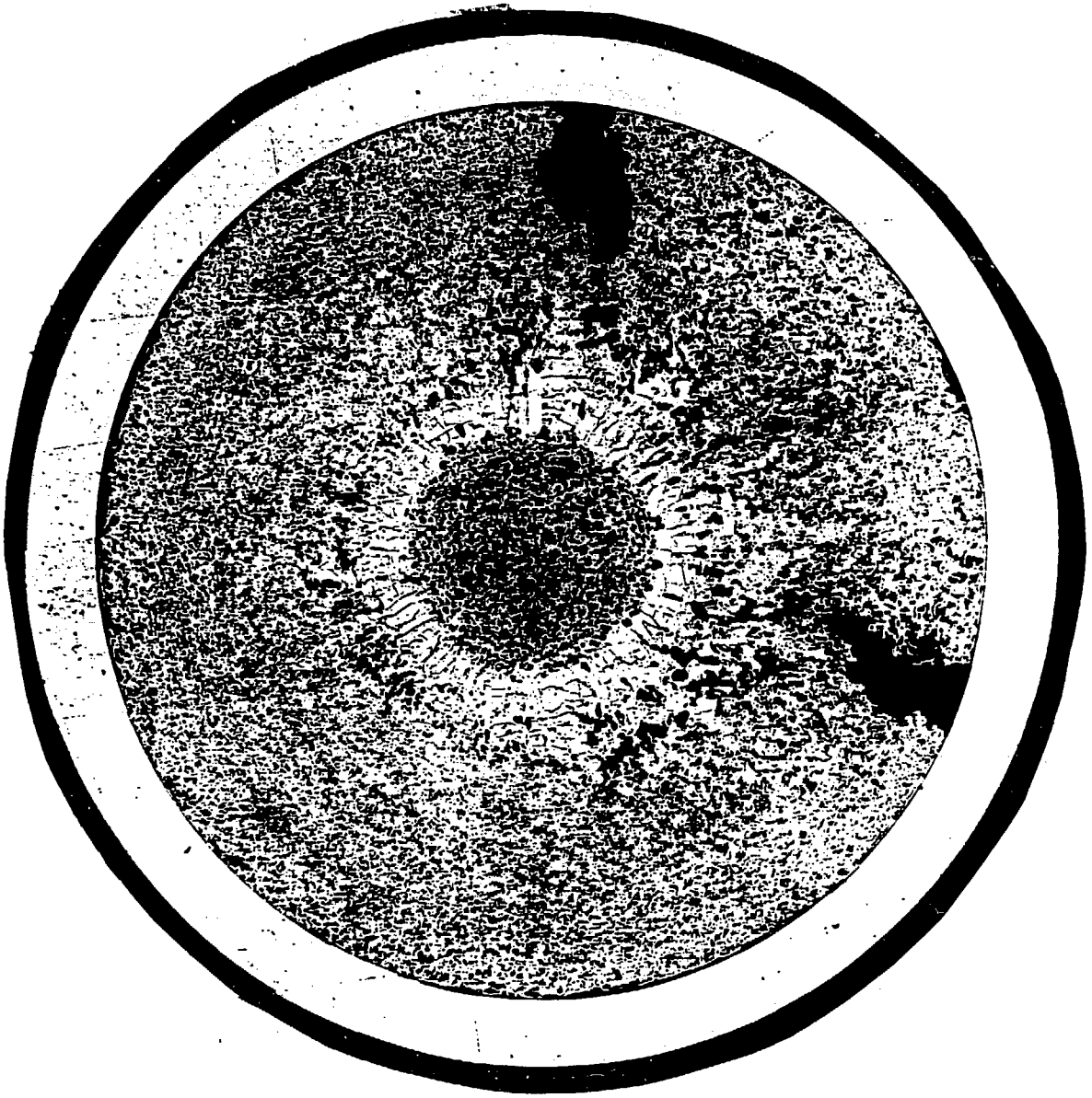

Figure 10 As-polished Microstructure of a U-19Pu-10Zr Slug Irradiated to ~3% Burnup Showing the Zirconium Depleted Annulus at Mid-radius.

U-19Pu-10Zr FUEL STRUCTURE AT TOP OF CORE AFTER 5.5 at.% BU

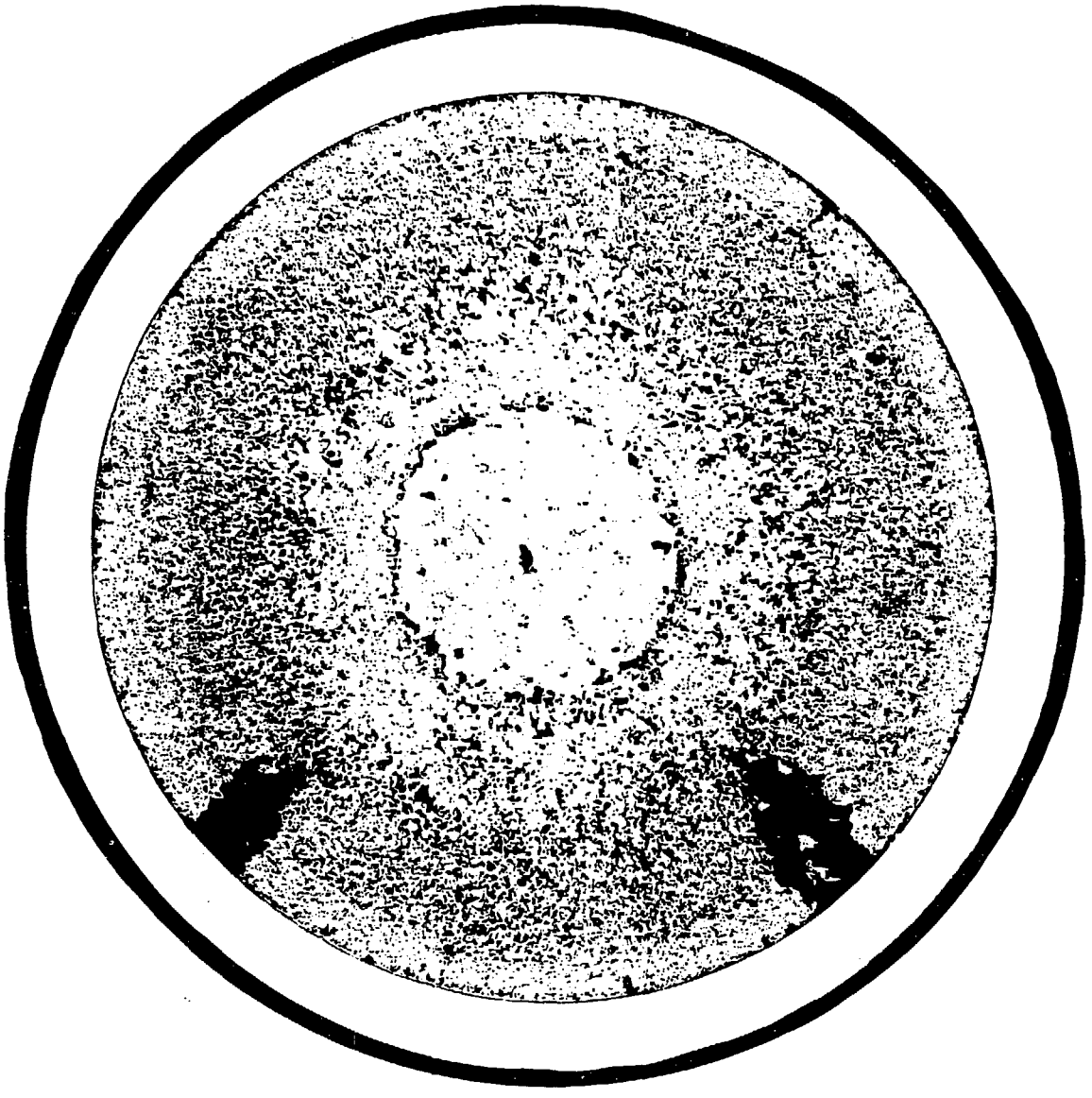

Figure 11 As-polished Microstructure of a U-19Pu-10Zr Slug Irradiated to 5.5% Burnup Showing the Zirconium Depleted Region at Fuel Centerline.

CLADDING CONTACT PROFILOMETRY

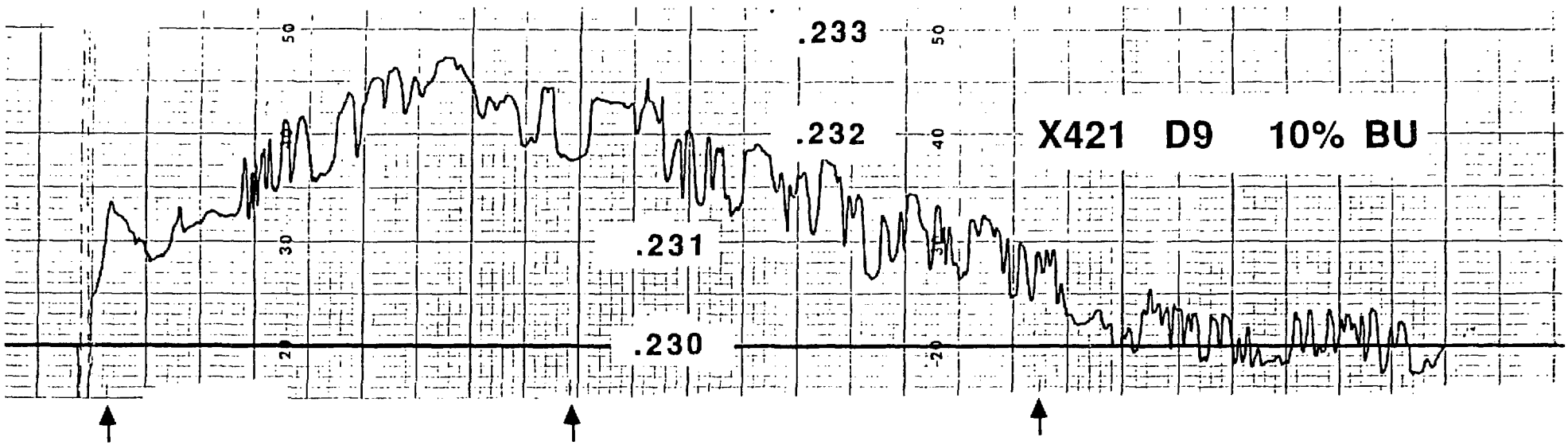

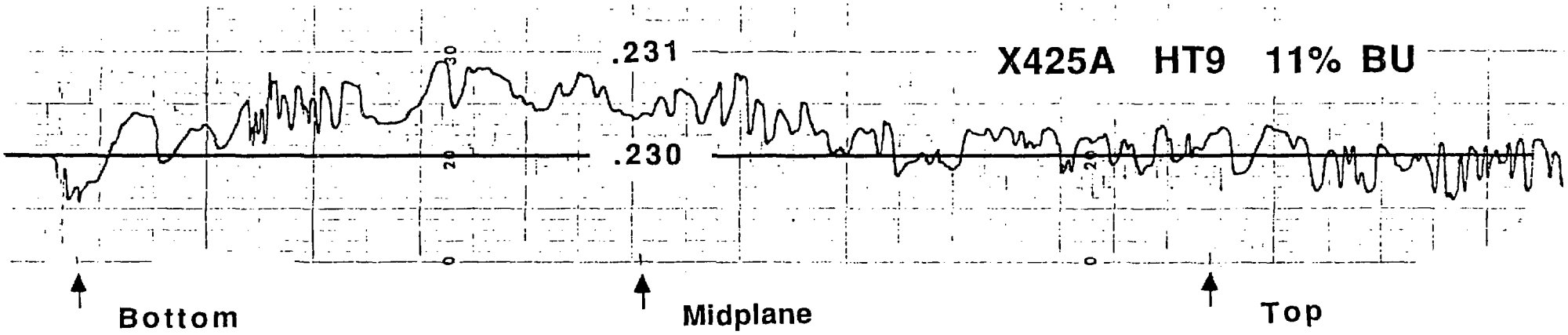

Figure 12 Comparison of D9 and HT9 Cladding Diametral Profiles After Burnups of 10-11% Burnup.

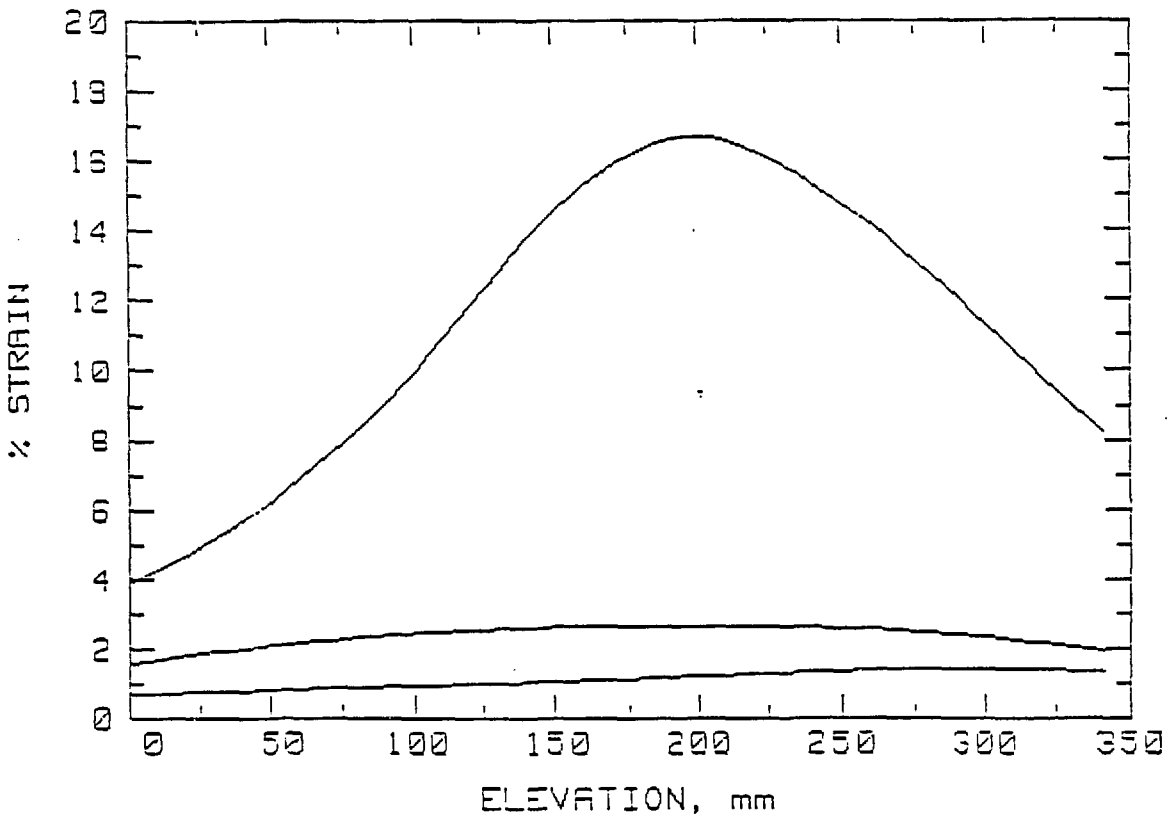

Figure 13 Calculations of Cladding Diametral Profiles of the 316 SS, D9, and HT9 Alloys After 15% Burnup.